International Journal of Recent Technology and Engineering (IJRTE)
ISSN: 2277-3878 (Online), Volume-8 Issue-6, March 2020

Synthesis and Microstructural Characterization of Cu_2MnSnS_4/Se_4 Nano-Thermoelectric Material

Hany R. Ammar, S. Sivasankaran, Abdulaziz S. Alaboodi

Abstract*: In the present study Cu_2MnSnS_4/Se_4 nanostructured material is synthesized using mechanical alloying. The elemental powders were alloyed in a high-energy ball mill under the following conditions: milling time 25 hours, ball-to-powder mass ratio (BPR) 10:1 and a rotation speed of 300 rpm. Detailed investigation of the microstructure of the synthesized alloy was carried out. The starting elemental powders size and morphology were characterized using Apreo field emission gun scanning electron microscope (FEGSEM). Elemental mapping of the synthesized alloy was characterized using energy dispersive spectroscopy (EDS) attached to FEGSEM system. Analysis of microstructure was performed using EDAX-TEAM advanced software. A dynamic laser light scattering was used for particle size analysis. The results showed that Cu_2MnSnS_4/Se_4 nanostructured is successfully synthesized by ball milling. The Z-average size distribution of the particle reveals that ball milling results in a considerable refining in the particle size from 44 micron down to 923.5 nm. Further, it was observed that 94.4% showed an average size of 725.8±233 nm. Microstructural analysis confirmed the formation of a homogenous structure of Cu_2MnSnS_4/Se_4 alloy in the powder and green samples. The elemental mapping confirmed the formation of solid solution of the processed alloy with homogenous distribution of all elements in the examined region. Quantitative analysis performed by EDAX-TEAM software confirmed the chemical composition and homogeneity of the processed material.

Keywords:* Cu_2MnSnS_4/Se_4 Alloy, Thermoelectric Materials, Ball Milling, Microstrucre Characterization.

I. INTRODUCTION

Presently, worldwide extraordinary research interest for utilization of renewable energy technology is aimed due to the dramatic climate change, exhausting of fossil fuels, and energy protective concerns. The present area of thermoelectric technology is one of the solid-state energy conversion technologies which change thermal energy to electricity directly using thermoelectric materials. According to Seebeck effect, the thermoelectric generator (TEG) is working in which voltage would generate when temperature differences occurs between hot and cold junction; this was invented by Thomas Seebeck in 1821 [1]. The main features of this technology are that there are no moving parts, compact in size, quite easy for operation, highly reliable and more over it is eco-friendly [2-7]. Though, this technology is limited as low in energy conversion efficiency. Therefore, nowadays researchers are concentrating to develop and get high energy conversion efficiency in thermoelectric materials by Nanotechnology.

Development along with improvement of thermoelectric properties can be explored and achieved through nanotechnology/nanomaterials. Hence, it is necessary to develop nano-thermoelectric materials that would improve the efficiency of thermoelectric generator for house hold and industrial appliances. Mostly, unidirectional solidification and/or powder metallurgy techniques are being used for the fabrication of thermoelectric materials. It was observed from researchers [8-10] that the thermoelectric materials produced from unidirectional solidification had offered poor mechanical strength due to large grain sizes even though it gives higher value of Fig. of merit (ZT) at room temperature. However, thermoelectric materials fabricated via hot-pressing technique had produced more mechanical strength due to full densification; but the performance results from thermoelectric materials were not up to the level.

The thermoelectric materials of n-type Bi2Te2.85Se0.15 developed by Svechnikova et al. [11] had reported that they had achieved Fig. of merit (ZT) value of ~0.93 (250-340 K) but low mechanical bending strength of 43MPa. One more thermoelectric material of Bi2Te2.85Se0.15 by Fan et al [12] had produced by ball milling and plasma-activated sintering technique. Based on these researchers, it can be identified that the mechanical alloying (MA) for synthesizing nano-thermoelectric materials would give more benefits for the fabrication of thermoelectric materials by which it is expected to get fine grain microstructure with improved thermoelectric along with mechanical properties.

The bulk dense Cu2SnSe3 thermoelectric materials with less than 2% porosity by self-sustained combustion reaction from elemental powders had successfully fabricated by Liu et al [13]. The authors found improvement in electrical conductivity of this material which was developed by partial substitution of Sn with In.

Manuscript received on March 12, 2020.
Revised Manuscript received on March 25, 2020.
Manuscript published on March 30, 2020.

* Correspondence Author
Hany R. Ammar*, Mechanical Engineering Department, Qassim University, Buraidah 51452, Saudi Arabia. Email: hanyammar@qec.edu.sa
Metallurgical and Materials Engineering Department, Faculty of Petroleum and Mining Engineering, Suez University, Suez, Egypt
S. Sivasankaran, Mechanical Engineering Department, Qassim University, Buraidah 51452, Saudi Arabia.Email: sivasankaran@qec.edu.sa
Abdulaziz S. Alaboodi, Mechanical Engineering Department, Qassim University, Buraidah 51452, Saudi Arabia. Email: alaboodi@qec.edu.sa

The Sn-doped thermoelectrical material and In-doped thermoelectric materials were produced Fig. of merit values of 0.51 and 0.62 at 773K, respectively.

PbS nanostructured thermoelectric materials were fabricated by Chang et al [14]. The main objectives of these authors were focused to reduce the value of lattice thermal conductivity. It was found that the PbS thermal conductivity decreased to around 0.50 Wm^{-1} K^{-1} as under nanostructured nature at the same temperature condition. Further, the authors were achieved the value of Fig. of merit (ZT) of 0.80 at 723 K. Mechanically sound (good strength) $Bi_2Te_{2.85}Se_{0.15}$ material was developed by Wang et al [15] in which the authors were used mechanical alloying for synthetization. Lie et al [16] were used combustion synthesis technique to enhance thermoelectric material properties on highly-dense $Cu_2ZnSnSe_4$ thermoelectric material. The authors found that the increased value of Fig. of merit for Cu2ZnSnSe4 thermoelectric sample was due to substitutional solid solution of Sn and In in the system. Si-Ge nanostructured based thermoelectric materials was synthesized by high-energy ball milling which was carried out by Usenko et al [17]. High configurational entropy with high thermal stability can be achieved by applying the concept of high-entropy alloys which is a multicomponent alloy. These high entropy alloys can be synthesized by severe plastic deformation technique of high-energy ball milling [18].

Based on several literatures, there is no work related to the development nanostructured Cu_2MnSnS_4/Se_4 thermoelectric materials prepared by high-energy mechanical alloying method. It is expected that this alloy to be a promising candidate for thermoelectric applications. This research paper will focus on synthesis and microstructural characterization of Cu_2MnSnS_4/Se_4 nanomaterials.

II. EXPERIMENTAL PROCEDURE

The as-received powders of pure elements (Cu, Mn, Sn, S and Se) with a minimum purity of 99.9% and an average particle size of -325 mesh/44µm were obtained from Nanografi Company, Turkey. The chemical composition of the fabricated sample is 16.8wt.% Cu, 8.3wt.% Mn, 8.3wt.% Sn, 33.3wt.% S and 33.3wt.% Se. These powders were mechanically alloyed using planetary mill Pulverisette 5/2 classic line. Tungsten-carbide (WC) vails of 250 ml capacity and WC balls of 10 mm diameter were used as grinding media. The mixed powders were milled for 25 hours with BPR of 10:1 and a rotation speed of 300 rpm. The milling was conducted in a liquid media of absolute ethanol (purity >99.99%). For the purpose of reducing the heat accumulation in the container, milling was performed in the sequence of 15 min clockwise rotation, pause for 15 min, anticlockwise rotation for 15 min and one more pause for 15 min, this cycle is repeated to achieve 25 hours of actual milling, as a continuous milling operation. The processed powders were then dried for microstructural analysis. Green samples were prepared using MTS universal test machine where the alloy powders were compacted in H13-steel die (15 mm inner-diameter) under a load of 400 MPa. The as-received elemental powders size and morphology were characterized using Apreo field emission gun scanning electron microscope (FEGSEM). Elemental mapping of the fabricated alloy in its powder and green compact forms was characterized using energy dispersive spectroscopy (EDS) attached to FEGSEM system. EDAX-TEAM advanced software was used for analyzing the microstructure of the sample. A dynamic laser light scattering (Malvern instrument) was used for measuring the average particle size of the fabricated alloy in its powder form.

III. RESULTS AND DISCUSSION

The average size of the starting elemental powders is -325mesh/44µm. The powders display different morphologies, as shown in Fig. 1. Copper reveals dendritic shape; manganese displays acicular/faceted fragments, sulfur shows asymmetrical nature, selenium reveals aggregated sphere-like morphology and tin has rounded shape.

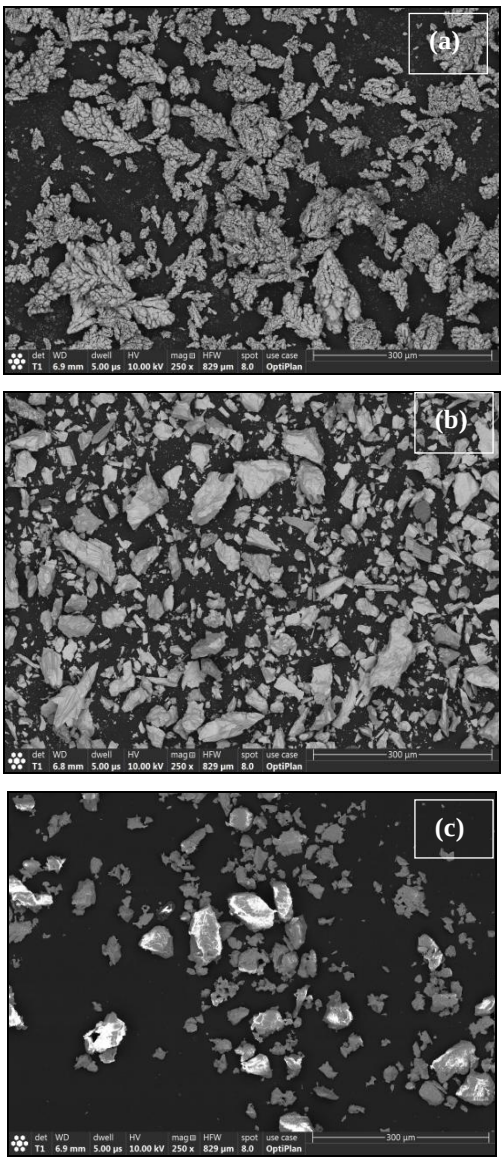

Retrieval Number: F9066038620/2020©BEIESP
DOI:10.35940/ijrte.F9066.038620
Journal Website: www.ijrte.org

Published By:
Blue Eyes Intelligence Engineering
& Sciences Publication

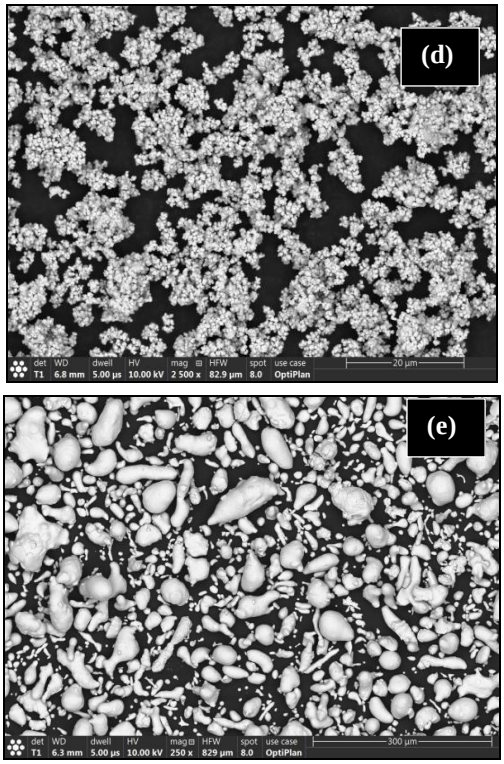

Fig. 1. The as-received powders shape and size: (a) Cu; (b) Mn; (c) S; (d) Se; and (e) Sn.

Fig. 2 shows the particle size distribution by intensity where the main peaks showed that the average particle size is 923.5 nm. The Z-average size distribution of the particle reveals that ball milling results in a considerable refining in particle size from 44 micron down to 923.5 nm. Further, it was observed that 94.4% showed an average size of 725.8±233 nm, as observed from the main peak in Fig. 2, this also gives an indication to the homogenous particle size obtained from milling process. Table I lists of the average particle size obtained from dynamic laser light scattering experiment.

Fig. 3 shows the microstructural characterization of Cu_2MnSnS_4/Se_4 alloy in its powder form after ball milling for 25 hours. The elemental mapping shown in Fig. 3 confirms the homogeneity of the alloy produced and the formation of a solid solution since uniform distribution of all elements could be observed through the examined area. Fig. 3(a) illustrates an overlay of the distribution of five elements (S, Sn, Mn, Cu, Se) used in production of Cu_2MnSnS_4/Se_4 thermoelectric materials. Fig. 3(b) shows the elemental distribution of sulfur; Fig. 3(c) displays the distribution of tin; Fig. 3(d) reveals the dispersion of manganese; Fig. 3(e) shows the map of copper; Fig. 3(f) displays the elemental dispersion of selenium. Fig. 4 shows the EDS sum spectrum as a plot of counts on vertical axis against energy range on horizontal axis, all elements in the synthesized alloy are well identified with a proper quantitative analysis, as shown in Table II.

For further analysis of the microstructure, the elemental mapping of a green sample is shown in Fig. 5 where the elements distribution in Cu_2MnSnS_4/Se_4 green sample is displayed. The elemental mapping shown in Fig. 5 further confirms the homogeneity of the alloy and the formation of a solid solution since more uniform distribution of all elements could be observed as compared to Fig. 3. The porosity level in the green sample is lower than that in the powder sample. Consequently, green sample displays better map in terms of homogeneity and the uniform dispersion of all elements. Fig. 5(a) illustrates an overlay of the dispersion of S, Sn, Mn, Cu and Se used in production of Cu_2MnSnS_4/Se_4 thermoelectric materials. Fig. 5(b) shows the elemental distribution of sulfur; Fig. 5(c) displays the distribution of tin; Fig. 5(d) reveals the dispersion of manganese; Fig. 5(e) shows the map of copper; Fig. 5(f) displays the elemental dispersion of selenium. Fig. 6 shows the EDS sum spectrum as a plot of counts against energy range, all elements in the fabricated alloy are well identified with appropriate quantitative analysis, as shown in Table III.

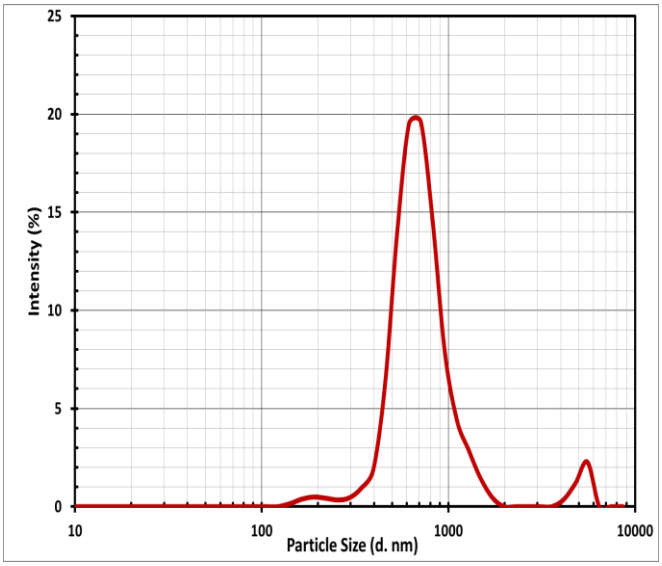

Fig. 2. The Z-average powders size distribution by intensity.

Table- I: Summary of the average particle size obtained from dynamic laser light scattering experiment.

Peak #	Size (d.nm)	% Intensity	Standard Deviation (d.nm)
Peak 1	725.8	94.4	233
Peak 2	5187	3.8	482.5
Peak 3	200	1.8	35.51
Z-Average (d.nm) = 923.5, PDI = 0.417			

Fig. 7 displays the results of a live map analysis of the green sample. Live map obtained from EDAX-TEAM software collects chemical composition of the selected region over the specimen in Fig. 7(a) and identify phase and elemental data, as shown in the map in Fig. 7(b). During the mapping process dynamic phase and elemental information will be displayed, as illustrated in Fig. 7(c). This live mapping is used to display phase to element or element to phase information, as summarized in Table IV which lists the live map analysis results of the green sample. In Table IV, phase composition in atomic % and the percent of each phase are listed. The live map results revealed a uniform dispersion of all elements with a complete solubility where all phases are containing S/Cu/Mn/Se/Sn with uniform dispersion in the selected region as shown from Fig. 7(b) and (c) and also listed in Table IV.

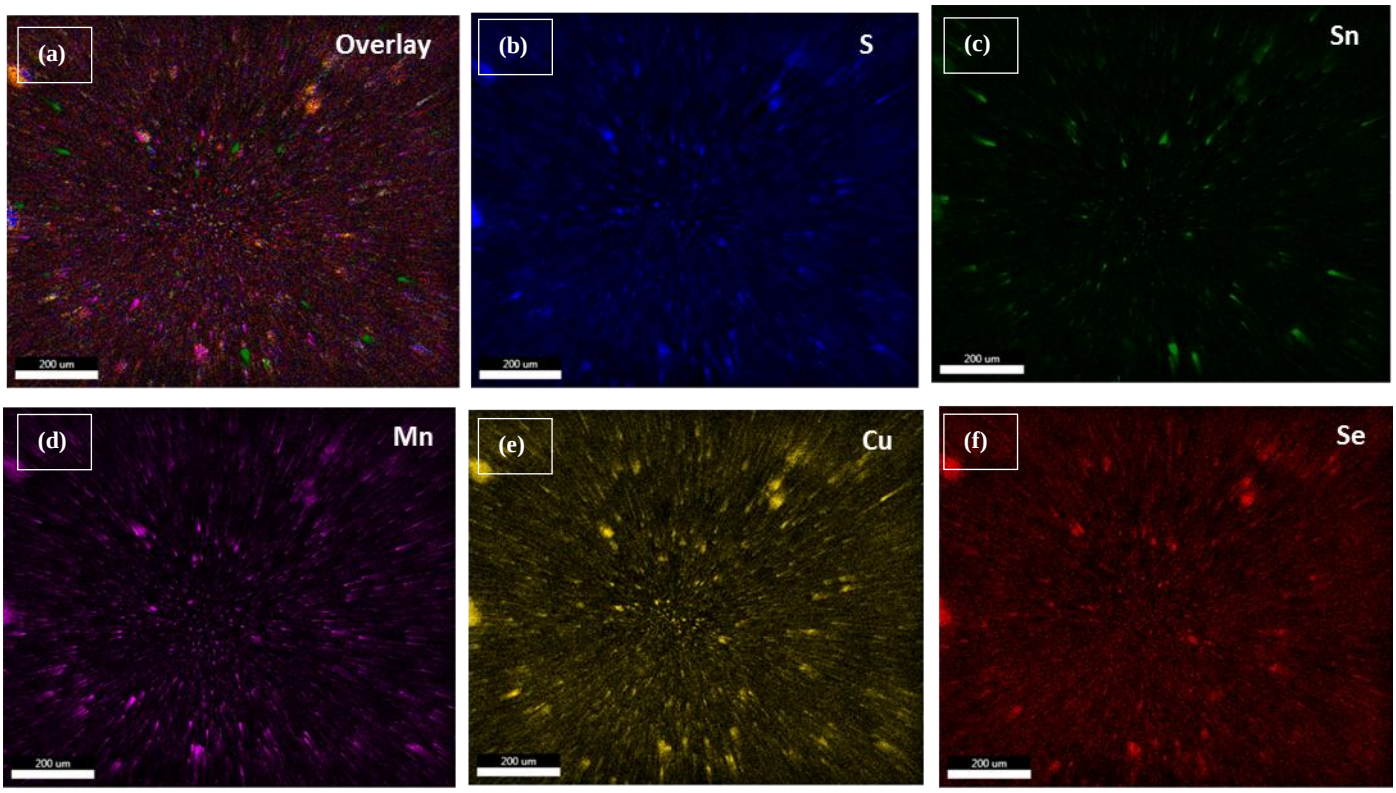

Fig. 3. Composition mapping of the powder sample: (a) an overlay of the distribution of five elements (S, Sn, Mn, Cu, Se); (b) S; (c) Sn; (d) Mn; (e) Cu; and (f) Se distribution through the selected region

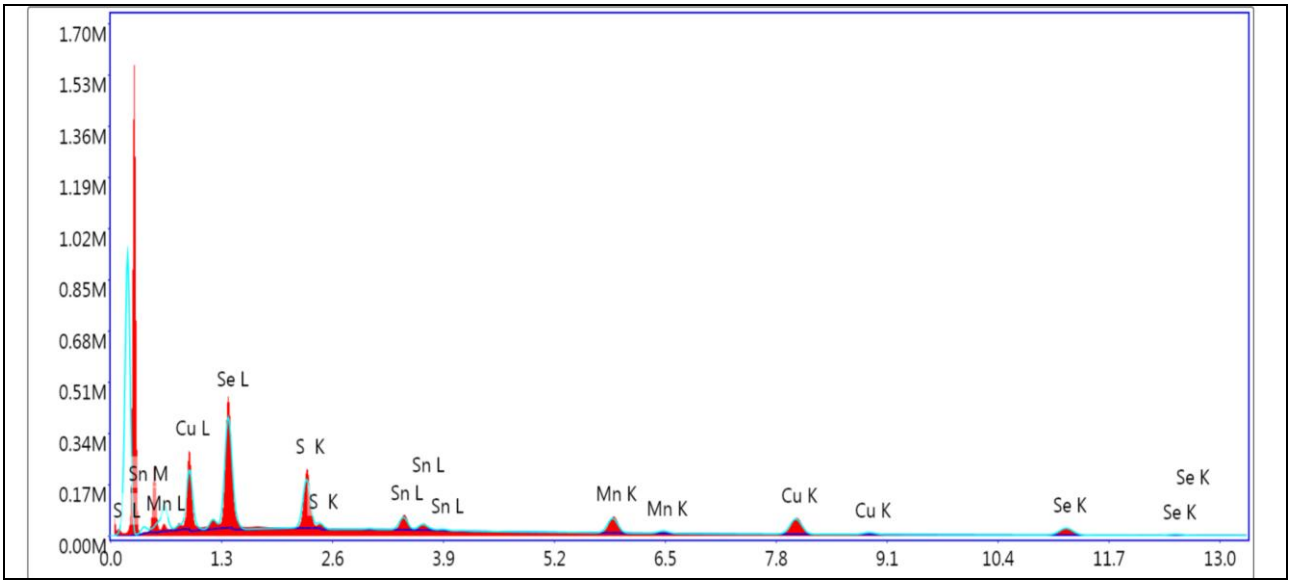

Fig. 4. EDS sum spectrum corresponding to the map region shown in Fig. 3.

Table- II: Quantitative analysis of the elements identified in the map region shown in Fig. 3.

Element	Weight%	Atomic%	Error%
S	13.25	25.79	1.68
Sn	8.98	4.72	1.38
Mn	10.17	11.56	1.53
Cu	23.47	23.05	1.92
Se	44.13	34.88	2.26

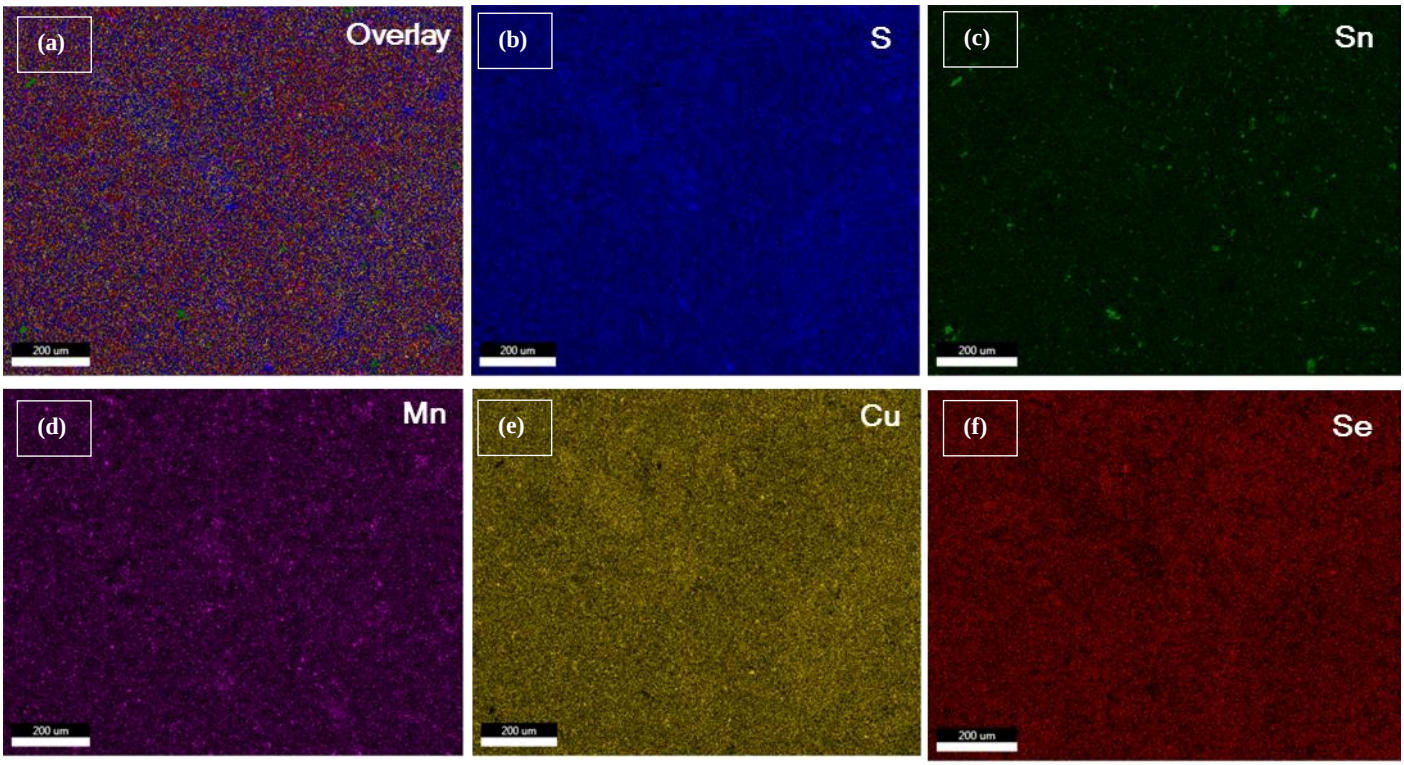

Fig.5. Composition mapping of the green sample: (a) an overlay of the distribution of five elements (S, Sn, Mn, Cu, Se); (b) S; (c) Sn; (d) Mn; (e) Cu; and (f) Se distribution through the selected region

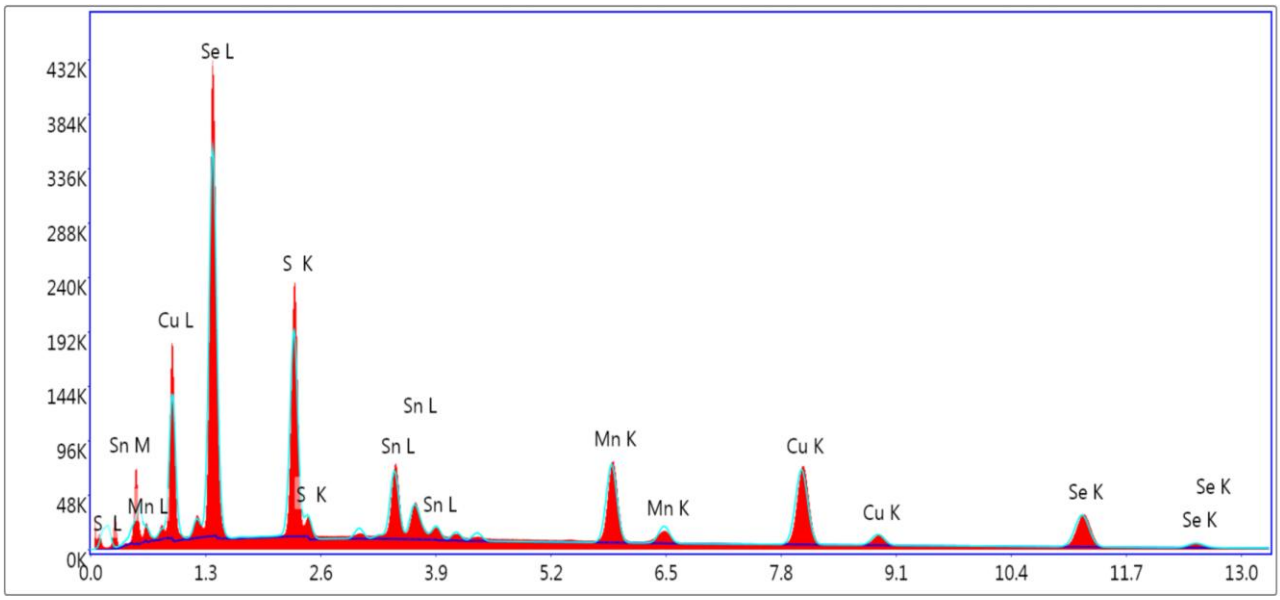

Fig. 6. EDS sum spectrum corresponding to the map region shown in Fig. 5.

Table- III: Quantitative analysis of the elements identified in the map region shown in Fig. 5.

Element	Weight%	Atomic%	Error%
S	13.29	25.97	1.79
Sn	12.35	6.52	1.23
Mn	12.08	13.77	1.45
Cu	22.41	22.09	1.73
Se	39.88	31.65	2.24

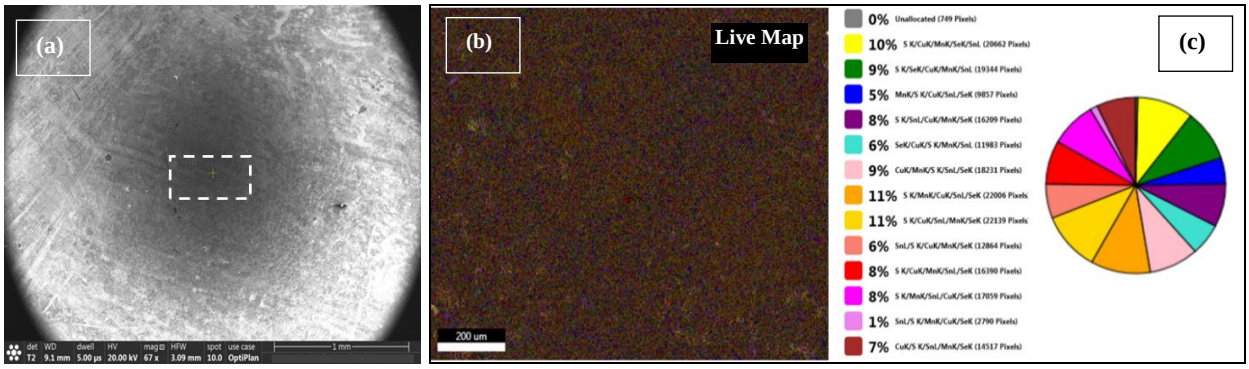

Fig.7. Live map analysis results: (a) the examined area in the green sample; (b) live map image; and (c) live map constituents.

Table-IV: Live map analysis results of green sample

Live Map Analysis Results	
Phase Composition in Atomic %	***% of the Phase***
(30.92)S-(4.78)Cu-(9.10)Mn-(30.93)Se-(24.27)Sn	10%
(23.15)S-(3.98)Se-(8.54)Cu-(14.89)Mn-(49.45)Sn	9%
(18.83)Mn-(5.10)S-(36.39)Cu-(15.59)Sn-(24.09)Se	5%
(32.91)S-(9.68)Sn-(10.90)Cu-(16.79)Mn-(29.73)Se	8%
(14.23)Se-(4.48)Cu-(8.95)S-(18.17)Mn-(54.17)Sn	6%
(20.12)Cu-(5.42)Mn-(19.11)S-(28.52)Sn-(26.82)	9%
(30.84)S-(6.03)Mn-(20.87)Cu-(18.94)Sn-(23.32)Se	11%
(28.30)S-(8.01)Cu-(10.88)Sn-(27.69)Mn-(25.11)Se	11%
(22.34)Sn-(11.92)S-(11.72)Cu-(21.98)Mn-(32.50)Se	6%
(40.77)S-(6.56)Cu-(10.01)Mn-(17.76)Sn-(24.90)Se	8%
(21.50)S-(7.68)Mn-(20.50)Sn-(15)Cu-()Se	8%
(18.28)Sn-(27.99)S-(11.35)Mn-(15.54)Cu-(26.84)Se	1%
(20.50)Cu-(5.73)S-(8.79)Sn-(35.49)Mn-(29.50)Se	7%

IV. CONCLUSIONS

In the present study Cu2MnSnS4/Se4 nanostructured material is synthesized using high-energy mechanical alloying. The powders were alloyed in a high-energy ball mill under the following conditions: milling time 25 hours, BPR 10:1 with a revolution of 300 rpm. Elemental mapping of the synthesized alloy was characterized using EDS attached to FEGSEM system. Analysis of microstructure was performed using EDAX-TEAM advanced software. The distribution of particle size was analyzed. The Cu_2MnSnS_4/Se_4 nanostructured is successfully synthesized by ball milling. The Z-average size distribution of the particle reveals that ball milling results in a considerable refining in the particle size from 44 micron down to 923.5 nm. Further, it was observed that 94.4% showed an average size of 725.8±233 nm. Microstructural analysis confirmed the formation of a homogenous structure of Cu_2MnSnS_4/Se_4 alloy in the powder and green samples. The elemental mapping confirmed the formation of solid solution of the processed alloy with homogenous distribution of all elements in the examined region. Quantitative analysis confirmed the chemical composition and homogeneity of the processed material.

ACKNOWLEDGEMENT

The authors gratefully acknowledge Qassim University, represented by the Deanship of Scientific Research, on the material support for this research under the number (3972-qec-2018-1-14-S) during the academic year 1437 AH/2016 AD.

REFERENCES

1. S.B. Riffat, X. Ma. Thermoelectrics: A review of present and potential applications. Appl. Therm. Eng, vol. 23, 2003, pp. 913-935.
2. L.E. Bell. Cooling, heating, generating power, and recovering waste heat with thermoelectric systems. Science, vol. 321, 2008, pp. 1457–1461.
3. J.P. Heremans, V. Jovovic, E.S. Toberer, et al. Enhancement of thermoelectric efficiency in PbTe by distortion of the electronic density of states. Science, vol. 31, 2008, pp. 554–557.
4. B. Poudel, Q. Hao, Y. Ma, et al. High-thermoelectric performance of nanostructured bismuth antimony telluride bulk alloys. Science, vol. 320, 2008, pp. 634–638.
5. A.I. Hochbaum, R.K. Chen, R.D. Delgado, et al. Enhanced thermoelectric performance of rough silicon nanowires. Nature, vol. 451, 2008, pp. 163–167.
6. H.K. Lyeo, A.A. Khajetoorians, L. Shi, Profiling the thermoelectric power of semiconductor junctions with nanometer resolution. Science, vol. 303, 2004, pp. 816–818.
7. M. Chen, H. Lund, L.A. Rosendahl, et al. Energy efficiency analysis and impact evaluation of the application of thermoelectric power cycle to today's CHP systems. Appl Energy vol. 87, 2010, pp. 1231–1238.
8. P.J. Taylor, J.R. Maddux, W.A. Jesser, F.D. Rosi, Room-temperature anisotropic, thermoelectric, and electrical properties of n-type (Bi2Te3)90 (Sb2Te3)5 (Sb2Se3)5 and compensated p-type (Sb2Te3)72 (Bi2Te3)25 (Sb2Se3)3 semiconductor alloys. J. Appl. Phys., vol. 85 1999, pp. 7807-7813.
9. W.M. Yim, F.D. Rosi, Compound tellurides and their alloys for peltier cooling-A review, Solid-State Electron, vol. 15(10), 1972, pp. 1121-1134.

10. J.Y. Yang, T. Aizawa, A. Yamamoto, T. Ohtab, Thermoelectric properties of n-type (Bi2Se3)x(Bi2Te3)1−x prepared by bulk mechanical alloying and hot pressing, J. Alloys Compd., vol. 312, 2000, pp. 326-330.
11. T.E. Svechnikova, P.P. Konstantinov, G.T. Alekseeva, Physical properties of Bi2Te2.85Se0.15 single crystals doped with Cu, Cd, In, Ge, S, or Se, Inorg. Mater., vol. 36(6), 2000, pp. 556-560.
12. X.A. Fan, J.Y. Yang, W. Zhu, H.S. Yun, R.G. Chen, S.Q. Bao, X.K. Duan, Microstructure and thermoelectric properties of n-type Bi2Te2.85Se0.15 prepared by mechanical alloying and plasma activated sintering, J. Alloys Compd., vol. 420, 2006, pp. 256-259.
13. Liu G, Chen K, Li J, Li Y, Zhou M, Li L, Combustion synthesis of Cu2SnSe3 thermoelectric materials, Journal of the European Ceramic Society, vol. 36, 2016, pp.1407-1415.
14. C. Chang, Y. Xiao, X. Zhang, Y. Pei, F. Li, S. Ma, B. Yuan, Y. Liu, S. Gong, L.D. Zhao, High performance thermoelectrics from earth-abundant materials: Enhanced figure of merit in PbS through nanostructuring grain size, Journal of Alloys and Compounds, vol. 664, 2016, pp. 411-416.
15. Z.L Wang, T. Akao, T. Onda, Z.C Chen, Microstructure and thermoelectric properties of hot-extruded Bi-Te-Se bulk materials, Journal of Alloys and Compounds, vol. 663, 2016, pp. 134-139.
16. G. Liu, J. Li, K. Chen, Y. Li, M. Zhou, Y. Han, L. Li, Direct fabrication of highly-dense Cu2ZnSnSe4 bulk materials by combustion synthesis for enhanced thermoelectric properties, Materials and Design, vol. 93, 2016, pp. 238-246.
17. A.A. Usenko, D.O. Moskovskikh, M.V. Gorshenkov, A.V. Korotitskiy, S.D. Kaloshkin, A.I. Voronina and V.V. Khovaylo, Optimization of ball-milling process for preparation of Si–Ge nanostructured thermoelectric materials with a high figure of merit, Scripta Materialia, vol. 96, 2015, pp. 9-12.
18. Yan et al., Suppression of the lattice thermal conductivity in NbFeSb-based half-Heusler thermoelectric materials through high entropy effects, Scripta Materialia, vol. 157, 2018, pp.129-134.

AUTHORS PROFILE

Hany R. Ammar, Assistant Professor, Mechanical Engineering Department, Qassim University, Saudi Arabia. More than 45 papers published in peer-review journals, the winner of the best paper award from the American Foundrymen Society 2011. Research area focus on synthesis and characterization. of advanced materials.

S. Sivasankaran, Associate Professor, Mechanical Engineering Department, Qassim University, Saudi Arabia. More than 65 papers published in peer-review journals. Research area focus on synthesis and characterization of nanomaterails.

Abdulaziz S. Alaboodi, Professor, Mechanical Engineering Department, Qassim University, Saudi Arabia. More than 45 papers published in peer-review journals. Research area focus on Finite Element Analysis and Nanotechnology.